Available online at www.sciencedirect.com
ScienceDirect
Ceramics International 36 (2010) 1137–1141
CERAMICS INTERNATIONAL
www.elsevier.com/locate/ceramint

Short communication

Fabrication of olivine-type $LiMn_xFe_{1-x}PO_4$ crystals via the glass–ceramic route and their lithium ion battery performance

Tsuyoshi Honma *, Kenta Nagamine, Takayuki Komatsu

Department of Materials Science and Technology, Nagaoka University of Technology, 1603-1 Kamitomioka-cho, Nagaoka 940-2188, Japan

Received 28 June 2009; received in revised form 3 September 2009; accepted 3 October 2009
Available online 4 November 2009

Abstract

The olivine-type $LiMn_xFe_{1-x}PO_4$ crystals are fabricated through the crystallization of Li_2O–MnO_2–Fe_2O_3–P_2O_5 glasses, and the lithium ion battery performance (electrochemical charge/discharge patterns) for the glass–ceramics with $LiMn_xFe_{1-x}PO_4$ crystals is examined. It is found that homogeneous glasses are obtained for the stoichiometric compositions corresponding to $LiMn_xFe_{1-x}PO_4$ with $0 \leq x \leq 0.8$ in a conventional melt-quenching method in air. The heat treatment of the mixtures of glass powders and glucose (5 wt%) at crystallization temperatures (~550 °C) in a reducing atmosphere of 7%H_2–93%Ar gives the formation of the olivine-type $LiMn_xFe_{1-x}PO_4$ crystals. The charge/discharge curves exhibit the plateaus at the voltage of ~3.4 and 4.1 V.

Keywords: B. Composites; C. Ionic conductivity; D. Glass ceramics; E. Batteries

1. Introduction

Lithium iron phosphate $LiFePO_4$ with an olivine structure has been proposed to be a potential candidate using cathode materials for the next generation of rechargeable lithium ion batteries [1,2]. $LiFePO_4$ cathode materials have a high theoretical capacity of 170 mAh/g, are environmentally benign, thermal stable in the fully charged state, and have low raw materials costs. Numerous studies reported so far suggest that the key points to achieve high performances as cathode materials are to control or design particle size, morphology, and interface between $LiFePO_4$ crystal particles. $LiFePO_4$ is commonly synthesized via solid-state reactions [1], hydrothermal methods [3], and so on. Recently, we proposed new routes for the fabrication of phosphate-based lithium ion battery related materials such as olivine-type $LiFePO_4$, Nasicon-like $Li_3Fe_2(PO_4)_3$, and β-$LiVOPO_4$, in which the technique of glass crystallization was applied [4–7].

$LiFePO_4$ has a poor electronic and ion conductivity, resulting in the poor rate performance and thus limiting commercial applications [8–14]. Many efforts have been made to improve the performance of $LiFePO_4$ cathode materials so far, including addition of conductive (Cu, Au, carbon) powders, doping of supervalence metal ions, carbon coating, and synthesis of nanoparticles [8–14]. The iron (Fe^{2+}) site in $LiFePO_4$ can be substituted with other transition metal ions such as Mn^{2+}, i.e., $LiMn_xFe_{1-x}PO_4$. In particular, it is noted that $LiMnPO_4$ having an olivine structure exhibits a plateau potential of 3.9 V in charge/discharge curves. This value of 3.9 V is higher than that (3.4 V) of $LiFePO_4$ [15,16].

In the glass–ceramic method, it is possible to synthesize target crystalline phase from homogeneous glassy phase and to design the size and morphology of crystalline phase through well-controlled crystal nucleation and growth. Because one of the most important points in practical applications of lithium ion secondary batteries based on the lithium iron phosphates is to establish simple processing methods with low cost, it is of interest and importance to apply a simple glass–ceramic method to materials having potentials as lithium ion secondary batteries. However, it should be emphasized that the application of glass–ceramic method to lithium ion secondary battery materials is extremely limited [4–7,17,18]. In particular, there have been no reports on the synthesis of $LiMnPO_4$ and Mn-doped $LiMn_xFe_{1-x}PO_4$ materials through glass–ceramic method. It should be also pointed out that there has been no information on the glass-formation and crystallization behavior

* Corresponding author. Tel.: +81 258 47 9312; fax: +81 258 47 9300.
E-mail address: honma@mst.nagaokaut.ac.jp (T. Honma).

0272-8842/$36.00
doi:10.1016/j.ceramint.2009.10.003

in the Li_2O–MnO_2–Fe_2O_3–P_2O_5. Usually, $LiMn_xFe_{1-x}PO_4$ crystals have been synthesized by solid-state reactions of raw materials such as $LiCO_3$, $MnCO_3$, $FeC_2O_4{\cdot}2H_2O$, and $NH_4H_2PO_4$ [15,16].

The purpose of this study is to fabricate olivine-type $LiMn_xFe_{1-x}PO_4$ crystals through the glass crystallization and to examine the lithium ion battery performance (electrochemical charge/discharge curves) for the glass–ceramics with $LiMn_xFe_{1-x}PO_4$ crystals. In this study, we clarified the glass-formation and crystallization behavior in the Li_2O–MnO_2–Fe_2O_3–P_2O_5 system, in particular for the stoichiometric compositions corresponding to $LiMn_xFe_{1-x}PO_4$, i.e., the $LiFePO_4$–$LiMnPO_4$ pseudo binary system. In previous studies [4,5], olivine-type $LiFePO_4$ crystals were crystallized in a glass with the composition of $26Li_2O$–$43FeO$–$5Nb_2O_5$–$26P_2O_5$, in which a small amount (5 mol%) of Nb_2O_5 was added to improve the glass-forming ability in Li_2O–FeO–P_2O_5 glasses. The present study is, therefore, different from the glass composition and the fabrication processing in previous studies [4,5,15,16].

2. Experimental

Glasses with the compositions of $LiMn_xFe_{1-x}PO_4$ in the Li_2O–MnO_2–Fe_2O_3–P_2O_5 system were prepared using a conventional melt-quenching method. Commercial powders of reagent grade $LiPO_3$, Fe_2O_3, MnO_2 were mixed well in a platinum crucible, and then the mixtures were melted at 1200 °C in an electric furnace for 15 min in air. The melts were poured onto an iron plate and pressed to a thickness of 0.5–1 mm by another iron plate. The glass transition, T_g, and crystallization peak, T_p, temperatures were determined using differential thermal analysis (DTA) at a heating rate of 10 K min^{-1}. Glass powders were obtained by crushing and grinding bulk plate glasses using a ball mill (Fritsch Co., Premium line P-7). Glucose was added to glass powders in order to reduce the valences of Fe^{3+} to Fe^{2+} and Mn^{4+} to Mn^{2+} during crystallization. The amount of glucose was 5 wt%. The mixtures of glass powders and glucose were heat treated at around temperatures crystallization peak temperature for 90 min in a reducing atmosphere of 7%H_2–93%Ar gas. The crystalline phase present in the crystallized samples was identified by X-ray diffraction (XRD) analyses (CuKα radiation) at room temperature. The concentration of Fe^{2+} in the glass and glass–ceramics with the composition of $LiFePO_4$ was determined using a cerium redox titration method, in which 0.1N-$Ce(SO_4)_2$ solution as titrant and ortho-phenanthoroline as indicator were used.

The electrochemical charge/discharge curves were measured using the following procedures: cathodes were prepared by mixing 80 wt% glass–ceramics obtained (i.e., active material), 15 wt% graphitic carbon, and 5 wt% polyvinylidene difluoride (PVDF). The mixture was then pressed into an Al thin sheet, and circular disks were prepared by cutting the sheet. Stainless test cells were constructed using a lithium metal anode and an electrolyte of 1 M $LiPF_6$ consisting of a 1:1 solution of ethylene carbonate (EC) and diethyl carbonate (DEC). The lithium ion battery performance at room temperature was evaluated from charge/discharge measurements (Hokuto denko Co., HJ-1001). The cell potential was swept in the voltage range of 2.5–4.5 V, and the charge/discharge rate was kept as C/10 in each cell.

3. Results and discussion

The XRD measurements for the melt-quenched samples with the nominal compositions of $LiMn_xFe_{1-x}PO_4$ were carried out. Only halo patterns were observed without any sharp peaks for the samples with $x = 0$–0.8, but the presence of crystals was confirmed for the samples with $x = 0.9$ and 1.0. The DTA curves for the melt-quenched samples with $x = 0$–0.8 are shown in Fig. 1. The endothermic peaks due to the glass transition and exothermic peaks due to the crystallization are clearly observed for all samples. These results indicate that the glass-forming region in the pseudo binary system of $(1-x)LiFePO_4$–$xLiMnPO_4$ is limited to the range of $x = 0$–0.8. As shown in Fig. 1, $LiMn_xFe_{1-x}PO_4$ glasses show the values of $T_g = 436$–497 °C and $T_p = 527$–568 °C. It should be pointed out that both T_g and T_p values decrease largely with the substitution of Mn ions for Fe ions. It was found from the cerium redox titration method that Fe ions in the glass ($LiFePO_4$) with $x = 0$ are present mainly as Fe^{3+} ions, i.e., $Fe^{3+}/(Fe^{2+} + Fe^{3+}) = 0.86$. Because the raw material of Fe_2O_3 was used for the glass preparation and the atmosphere in the melting was air in the present study, this result would be reasonable. At this moment, the valence state of Mn ions in $LiMn_xFe_{1-x}PO_4$ glasses has not been determined. It is, however, expected that Mn ions would take the valences of Mn^{3+} and Mn^{4+} in the glasses, because MnO_2 was used as raw material.

As seen in Fig. 1, the difference between the glass transition and crystallization temperatures, i.e., $\Delta T = T_p - T_g$, in $LiMn_xFe_{1-x}PO_4$ glasses varies depending on the Mn/Fe ratio. For instance, the values were obtained $\Delta T = 71$ K for $LiFePO_4$

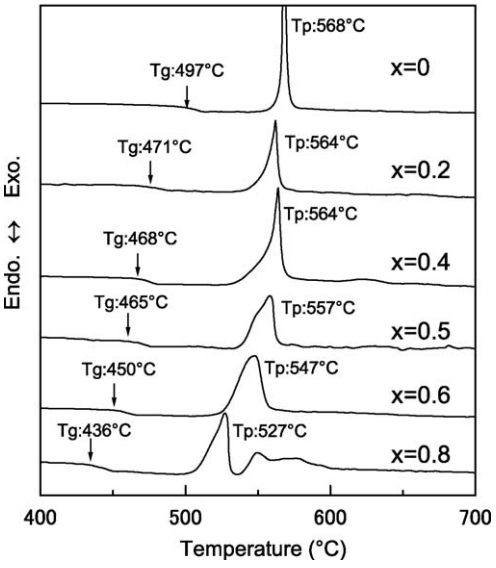

Fig. 1. DTA curves for the melt-quenched bulk samples with the compositions of $LiMn_xFe_{1-x}PO_4$ ($0 < x < 0.8$). The heating rate was 10 K min^{-1}.

glass, $\Delta T = 96$ K for $LiMn_{0.4}Fe_{0.6}PO_4$ glass, and $\Delta T = 91$ K for $LiMn_{0.8}Fe_{0.2}PO_4$ glass. It is known that the value of $\Delta T = T_p - T_g$ is a good estimation for the thermal stability against crystallization in glasses, i.e., the glass-forming ability. The results shown in Fig. 1, therefore, suggest that the glass-forming ability in the Li_2O–Fe_2O_3–P_2O_5 system is enhanced by addition of MnO_2. As will be described in below, Mn ions are incorporated into $LiFePO_4$ crystals and the formation of $LiMn_xFe_{1-x}PO_4$ crystals is confirmed. In previous studies [4,5], it was confirmed that the addition of a small amount (5 mol%) of Nb_2O_5 is effective in improving the glass-forming ability of lithium iron phosphate glasses, but Nb ions donot incorporate into $LiFePO_4$ crystals, consequently inducting the precipitation of $Li_3Nb_3O_8$ crystals as a byproduct together with $LiFePO_4$ crystals in the glass crystallization. The addition of Mn ions is more attractive in the points of glass-formation and crystallization in lithium iron phosphate glasses compared with Nb ions.

The powder XRD patterns for the samples (glass–ceramics) obtained by heat treatments at the crystallization peak temperature for 90 min in 7%H_2–93%Ar gas are shown in Fig. 2, where the mixtures of $LiMn_xFe_{1-x}PO_4$ glass powders (average grain size = 2 μm) and 5 wt% glucose were crystallized. All diffraction peaks were assigned to the olivine-type $LiMn_xFe_{1-x}PO_4$ crystalline phase. It is noted that any other crystalline phases such as $Li_3Fe_2(PO_4)_3$ have not been detected. It was also found from the cerium redox titration method that Fe ions in the crystallized sample ($LiFePO_4$) with $x = 0$ are present mainly as Fe^{2+} ions, i.e., $Fe^{2+}/(Fe^{2+} + Fe^{3+}) = 0.87$. That is, Fe^{3+} ions present in the precursor glasses are reduced significantly to Fe^{2+} ions during the crystallization.

The lattice parameters of $LiMn_xFe_{1-x}PO_4$ crystals formed in the crystallized samples (glass–ceramics) were estimated using

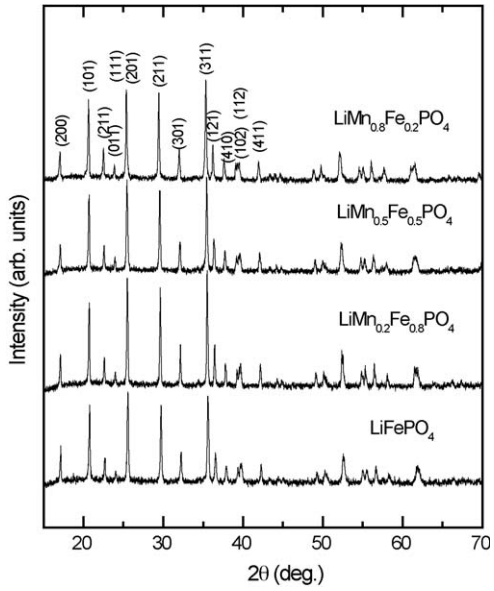

Fig. 2. Powder XRD patterns for the samples (glass–ceramics) obtained by heat treatments at the crystallization peak temperature for 90 min in a reducing atmosphere of 7%H_2–93%Ar. The mixtures of $LiMn_xFe_{1-x}PO_4$ glass powders (average grain size = 2 μm) and 5 wt% glucose were crystallized.

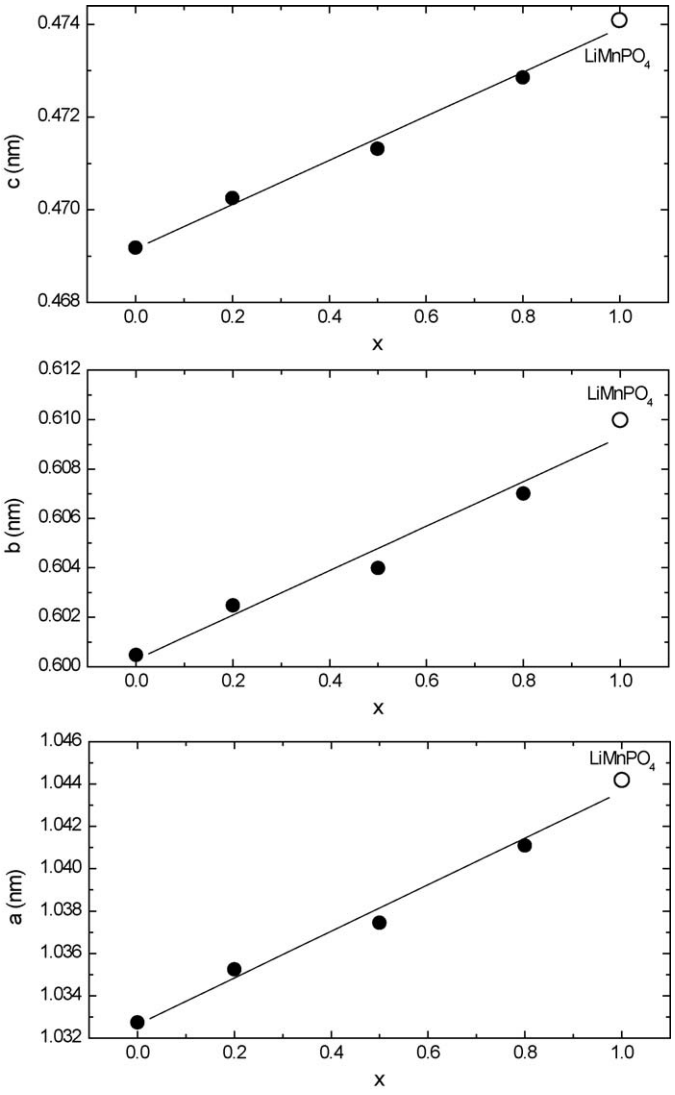

Fig. 3. Lattice constants of $LiMn_xFe_{1-x}PO_4$ crystals formed in the crystallized samples (glass–ceramics) obtained by heat treatments at the crystallization peak temperature for 90 min in a reducing atmosphere of 7%H_2–93%Ar.

Rietveld method, and the results are shown in Fig. 3. For instance, the values of $a = 1.033$ nm, $b = 0.6005$ nm, and $c = 0.4692$ nm for $LiFePO_4$ crystals were obtained. Padhi et al. [1] reported the lattice parameters of $a = 1.0334$ nm, $b = 0.6008$ nm, and $c = 0.4693$ nm for $LiFePO_4$ crystals which were synthesized by a conventional solid-state reaction. It is, therefore, concluded that olivine-type stoichiometric $LiFePO_4$ crystals are formed even in the crystallization of the precursor $LiFePO_4$ glass. As shown in Fig. 3, the lattice constants of $LiMn_xFe_{1-x}PO_4$ crystals increase almost linearly with increasing Mn content. The ionic radii of Fe^{2+} and Mn^{2+} ions in the six oxygen coordinated state are 0.061 and 0.067 nm, respectively [19]. Very recently, Bramnik and Eherenberg [20] have reported the lattice parameters of $a = 1.0442$ nm, $b = 0.6100$ nm, and $c = 0.4741$ nm for olivine-like $LiMnPO_4$ crystals which were synthesized from the $NH_4MnPO_4{\cdot}H_2O$ precursor precipitated from the aqueous solution. Those values are plotted in Fig. 3. It is seen that the lattice constants for

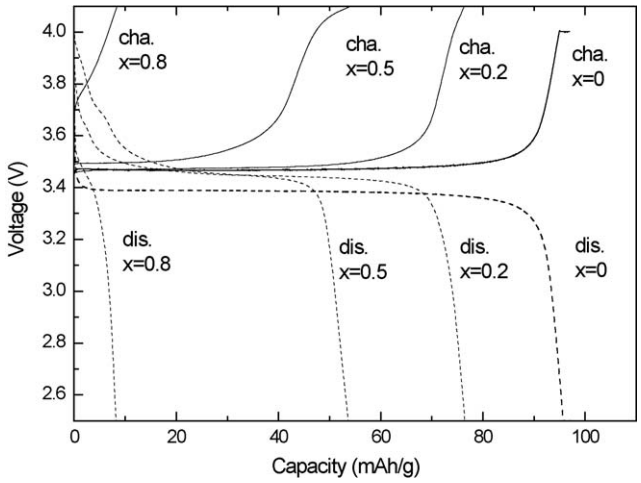

Fig. 4. Electrochemical charge and discharge curves for the cells consisting of $LiMn_xFe_{1-x}PO_4$ glass–ceramics as the cathode and lithium metal as the anode. The cell potential was swept in the voltage range of 2.5–4.5 V, and the charge/discharge rate was kept as C/10 in each cell.

$LiMn_xFe_{1-x}PO_4$ crystals formed in the crystallized samples (present study) change nearly depending on the Vegard's law between $LiFePO_4$ and $LiMnPO_4$ crystals. These results strongly suggest that the ratio of Mn^{2+}/Fe^{2+} in $LiMn_xFe_{1-x}PO_4$ crystals formed through the crystallization is very close to the ratio of Mn^{2+}/Fe^{2+} in the precursor glasses. The formation of $LiMn_xFe_{1-x}PO_4$ crystals also indicate that the reduction of Mn^{3+} and Mn^{4+} to Mn^{2+} is taking place during the crystallization. That is, glucose added to the glass powders is acting as a reducing agent not only for Fe^{3+} ions but also for Mn^{3+} and Mn^{4+} ions.

The electrochemical charge and discharge curves for the cells consisting of $LiMn_xFe_{1-x}PO_4$ glass–ceramics as the cathode and lithium metal as the anode. As shown in Fig. 4 the charging curve for $LiMn_{0.5}Fe_{0.5}PO_4$ glass–ceramics shows a clear plateau at 3.4 and 4.1 V, which represents red/ox potentials of Fe^{3+}/Fe^{2+} and Mn^{3+}/Mn^{2+}. In other $LiMn_xFe_{1-x}PO_4$ glass–ceramics, a clear plateau is not observed at 4.1 V. The electrochemical capacity decreases with increasing Mn content. A similar tendency has been observed for $LiMn_xFe_{1-x}PO_4$ crystals prepared by other methods [1,8]. Yamada et al. [9] reported that $LiMn_{0.6}Fe_{0.4}PO_4$ crystals exhibit the charge/discharge capacity of 160 mAh/g under a high-rate (C/2).

As demonstrated in the present study, $LiMn_xFe_{1-x}PO_4$ crystals are synthesized through the crystallization of glasses and glass–ceramics with $LiMn_xFe_{1-x}PO_4$ crystals show lithium ion battery properties, although the charge/discharge capacity is small. Further studies on the carbon coating and morphology of $LiMn_xFe_{1-x}PO_4$ crystals prepared by the glass crystallization method would be necessary to improve lithium ion battery performances.

4. Conclusion

The glasses with the compositions of $LiMn_xFe_{1-x}PO_4$ ($0 \leq x \leq 0.8$) in the Li_2O–MnO_2–Fe_2O_3–P_2O_5 system were prepared using a conventional melt-quenching method in air, and the glass–ceramics consisting of the olivine-type $LiMn_xFe_{1-x}PO_4$ crystals were fabricated through the crystallization in a reducing atmosphere of 7%H_2–93%Ar. The substitution of Mn ions for Fe ions was found to be effective in enhancing the glass-forming ability. It was found that glucose is a good agent for the reduction of Fe^{3+} to Fe^{2+} and Mn^{3+} and Mn^{4+} to Mn^{2+} during the crystallization. The lithium ion battery performance (electrochemical charge/discharge patterns) for the glass–ceramics with $LiMn_xFe_{1-x}PO_4$ crystals was examined, and the plateaus at the voltage of ~3.4 and 4.1 V were observed in the charge/discharge curves.

Acknowledgement

This work was supported from the Grant-in-Aid for Scientific Research from the Ministry of Education, Science, Sports, Culture, and Technology, Japan.

References

[1] A.K. Padhi, K.S. Nanjundaswamy, J.B. Goodenough, Phospho-olivines as positive-electrode materials for rechargeable lithium batteries, J. Electrochem. Soc. 144 (1997) 1188–1194.
[2] A.K. Padhi, K.S. Nanjundaswamy, C. Masquelier, S. Okada, J.B. Goodenough, Effect of structure on the Fe^{3+}/Fe^{2+} redox couple in iron phosphates, J. Electrochem. Soc. 144 (1997) 1609–1613.
[3] S. Yang, P.Y. Zavalij, M.S. Whittingham, Hydrothermal aynthesis of lithium iron phosphate cathodes, Electrochem. Commun. 3 (2001) 505–508.
[4] K. Hirose, T. Honma, Y. Benino, T. Komatsu, Glass–ceramics with $LiFePO_4$ crystals and oriented crystal line patterning in glass by YAG laser irradiation, Solid State Ionics 178 (2007) 801–807.
[5] K. Hirose, T. Honma, Y. Doi, Y. Hinatsu, T. Komatsu, Moessbauer analysis of Fe ion state in lithium iron phosphate glasses and their glass–ceramics with olivine-type $LiFePO_4$ crystals, Solid State Commun. 146 (2008) 273–277.
[6] K. Nagamine, K. Hirose, T. Honma, T. Komatsu, Lithium ion conductive glass–ceramics with $Li_3Fe_2(PO_4)_3$ and YAG laser-induced local crystallization in lithium iron phosphate glasses, Solid State Ionics 179 (2008) 508–515.
[7] K. Nagamine, T. Honma, T. Komatsu, Selective synthesis of lithium ion conductive β-$LiVOPO_4$ crystals via glass–ceramic processing, J. Am. Ceram. Soc. 91 (2008) 3920–3925.
[8] H. Huang, S.C. Yin, L.F. Nazar, Approaching theoretical capacity of $LiFePO_4$ at room temperature at high rates, Electrochem. Solid State Lett. 4 (2001) A170–A172.
[9] A. Yamada, S.C. Chung, K. Hinokuma, Optimized $LiFePO_4$ for lithium battery cathodes, J. Electrochem. Soc. 148 (2001) A224–A229.
[10] N. Ravet, Y. Chouinard, J.F. Magnan, S. Besner, M. Gauthier, M. Armand, Electroactivity of natural and synthetic triphylite, J. Power Sources 97–98 (2001) 503–507.
[11] P.P. Prosini, D. Zanc, M. Pasquali, Improved electrochemical performances of a $LiFePO_4$-based composite cathode, Electrochim. Acta 46 (2001) 3517–3523.
[12] S.Y. Chung, J.T. Bloking, Y.M. Chinag, Electronically conductive phosphor-olivines as lithium storage electrodes, Nature Mater. 1 (2002) 123–128.
[13] Z. Chen, J.R. Dahn, Reducing carbon in $LiFePO_4$/C composite electrodes to maximize specific energy, volumetric energy, and tap density, J. Electrochem. Soc. 149 (2002) A1184–A1189.
[14] F. Croce, A.D. Epifanio, J. Hassoun, A. Deptula, T. Olczac, B. Scrosati, A novel concept for the synthesis of an improved $LiFePO_4$ lithium battery cathode, Electrochem. Solid State Lett. 5 (2002) A47–A50.

[15] A. Yamada, M. Hosoyo, S. Chung, Y. Kudo, K. Hinokuma, K. Liu, Y. Nishi, Olivine-type cathodes: achievements and problems, J. Power Sources 119–121 (2003) 232–238.

[16] C.M. Burba, R. Frech, Local structure in the Li-ion battery cathode material $Li_x(Mn_yFe_{1-y})PO_4$ for $0 < x \leq 1$ and $y = 0.0$, 0.5 and 1.0, J. Power Sources 172 (2007) 870–876.

[17] J.C. Zheng, X.H. Li, Z.X. Wang, H.J. Guo, S.Y. Zhou, $LiFePO_4$ with enhanced performance synthesized by a novel synthetic route, J. Power Sources 184 (2008) 574–577.

[18] P. Jozwiak, J. Garbarczyk, F. Gendron, A. Mauger, C.M. Julien, Disorder in Li_xFePO_4: from glasses to nanocrystallites, J. Non-Cryst. Solids 354 (2008) 1915–1925.

[19] R.D. Shannon, Revised effective ionic radii and systematic studies of interatomic distances in halides and chalcogenides, Acta Cryst. A 32 (1976) 751–767.

[20] N.N. Bramnik, H. Eherenberg, Precursor-based synthesis and electrochemical performance of $LiMnPO_4$, J. Alloy Compd. 464 (2008) 259–264.